Scanning Probe Spectroscopy

R. Heer, G. Ploner, D. Rakoczy, J. Smoliner, G. Strasser

Institut für Festkörperelektronik, Technische Universität Wien, Floragasse 7, A-1040 Vienna, Austria

1. Magnetic field effects in $k_{//}=0$ filtering structures for BEEM experiments

(J. Smoliner, R. Heer, G. Strasser)

Until now, only little attention was paid to the situation where electrons are transferred between areas of different effective mass, since it seems to need a combination of locally varying effective mass and low dimensional states in order to observe some interesting physical effects. A field of research where electron transfer between areas of different effective mass plays an especially important role is Ballistic Electron Emission Microscopy (BEEM). BEEM is a three terminal extension of conventional scanning tunneling microscopy (STM), where ballistic electrons are injected from a STM tip into a semiconductor (GaAs, $m^*=0.067m_0$) via a thin metal base layer ($m^*=m_0$) evaporated onto the sample.

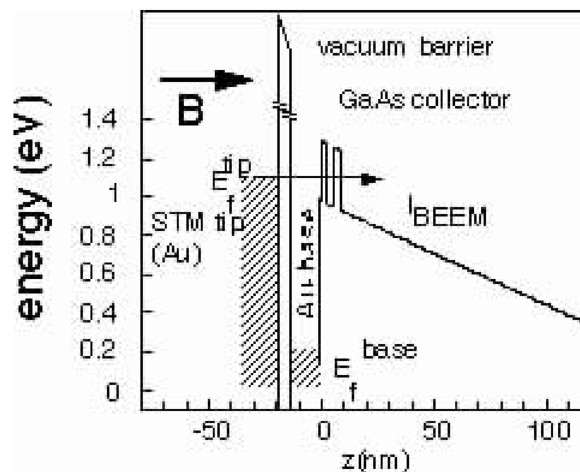

Fig. 1: Setup of the experiment.

As we have shown earlier, GaAs-AlGaAs double barrier resonant tunneling structures directly grown below the sample surface exhibit characteristic step-like features in the BEEM spectrum. Qualitatively, this effect is due to electron "refraction" at the Au-GaAs interface in combination with the resonant tunneling process through the states inside the double barrier structures. To describe the observed effect in a quantitative way, an extended Transfer Matrix Method (TMM) was introduced. We have found, that at interfaces between regions of different effective mass, the transmission coefficient for ballistic electrons becomes a function both of $E_\perp$ and $k_{//}$ and that sub surface resonant tunneling structures act as $k_{//}$ filters for electrons close to $k_{//} = 0$. In this way, the typical

steplike behavior of the BEEM spectrum can be explained. To investigate the $k_{//}$ filtering behavior in more detail, BEEM measurements were carried out in magnetic fields applied perpendicular to the sample. As one can see, the BEEM spectrum is strongly influenced by the magnetic field. The step can be quenched and even double steps can occur at certain fields. If the bias is fixed and the magnetic field is varied, it becomes obvious that the ballistic current oscillates independently for each value of V_t.

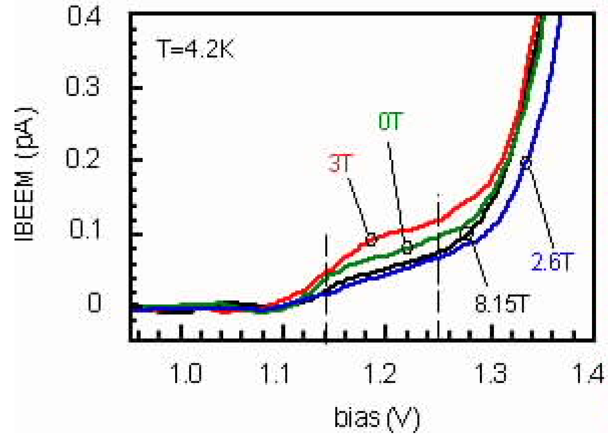

Fig. 2: Typical BEEM spectrum obtained on sub-surface resonant tunneling diodes for various magnetic fields. The measurement was carried out in liquid helium.

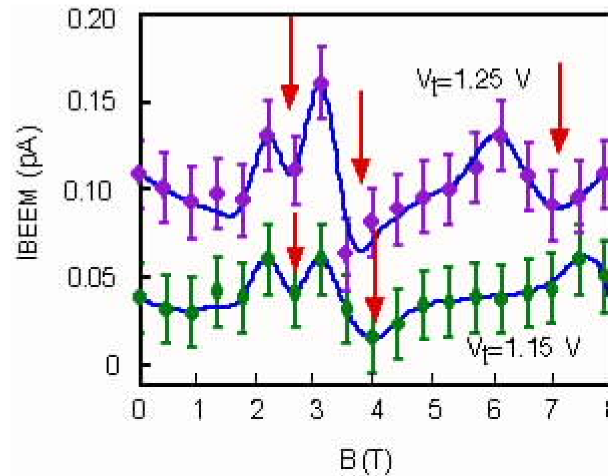

Fig. 3: BEEM current as a function of magnetic field and tunneling bias.

This behavior comes clear if the $k_{//}$ filtering effect is taken into account. If our structure really acts as filter for electrons close to $k_{//} = 0$ or $E_{//} = 0$, the oscillatory behavior can be explained in analogy to the Shubnikov de-Haas effect in two-dimensional electron gas systems: In magnetic fields, Landau level will exist inside the resonant tunneling diode. If the field is increased, the level spacing increases, too, and the number of levels inside the allowed $E_{//}$ range will decrease. As each allowed Landau level carries a part of the BEEM current, a minimum in the BEEM current an be expected each time a Landau level is shifted outside the allowed energy range.

2. GaAs cap layers in ballistic electron transport through GaAs-AlGaAs RTD's

(R. Heer, J. Smoliner, G. Ploner, G. Strasser)

Until now, only little attention was paid to the situation where electrons are transferred between areas of different effective mass, since it seems to need a combination of locally varying effective mass and low dimensional states in order to observe some interesting physical effects. On InAs-AlSb resonant tunneling diodes, e.g., this is the case and it was found that the calculated current voltage characteristics differs qualitatively from the experimental data because the longitudinal and transversal components of the electron wave vectors are coupled on these samples.

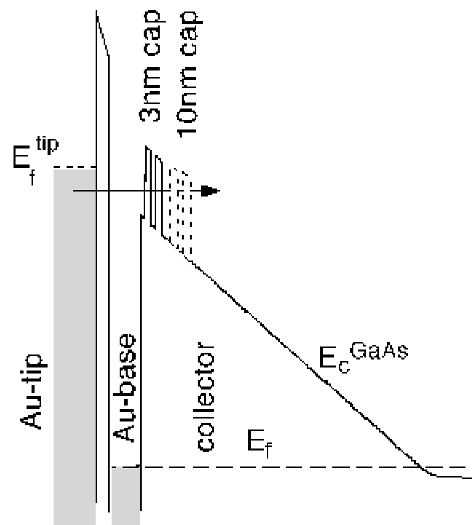

Fig. 4: Schematic setup, the thickness of the cap layer is modulated by wire etching.

A field of research where electron transfer between areas of different effective mass plays an especially important role is Ballistic Electron Emission Microscopy (BEEM). BEEM is a three terminal extension of conventional scanning tunneling microscopy (STM), where ballistic electrons are injected from a STM tip into a semiconductor (GaAs, $m^* = 0.067\ m_0$) via a thin metal base layer ($m^* = m_0$) evaporated onto the sample. In our group, the energetic distribution of ballistic electrons in GaAs is studied employing buried GaAs-AlGaAs resonant tunneling structures as energy filter in BEEM experiments. The conduction band diagram is shown in Fig. 4 in the configuration of the 10 nm cap layer.

Due to the large difference in electron mass in the Au base electrode and the GaAs collector, we found that parallel momentum conservation leads to considerable electron refraction at the Au-GaAs interface, and as a consequence, an almost linear behavior of the BEEM spectrum is observed in the energetic regime below the AlGaAs barrier height, as shown in Fig. 5 curve (A). Buried GaAs-AlGaAs resonant tunneling structures acts as an energy filter in BEEM experiments for $E_\perp$. GaAs-AlGaAs double barrier resonant tunneling structures grown directly below the sample surface exhibit characteristic step-like features in the BEEM spectrum and act as parallel momentum filter for ballistic electrons at $k_{//} = 0$, as shown in Fig. 5 curve (B).

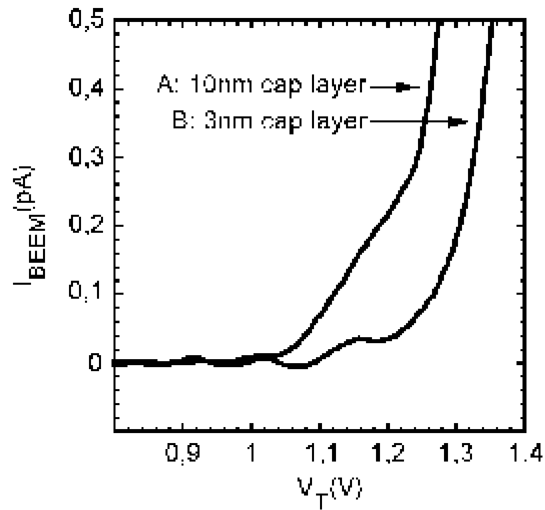

Fig. 5: BEES data obtained on top of the wire (A) and in the valley (B) @ 4,2K. Curve (A) shows a linear behavior, curve (B) shows a step-like feature in the region of the RTD barriers, respectively. Since the tunneling current in curve (A) was 5 nA and in curve (B) was 2 nA, the step-like feature is somehow less pronounced.

Qualitatively, this effect is due to electron refraction at the Au-GaAs interface in combination with the resonant tunneling process through the states inside the double barrier structures. To describe the observed effect in a quantitative way, an extended Transfer Matrix Method (TMM) is used. It shows that at interfaces between regions of different effective mass, the transmission coefficient for ballistic electrons becomes a function both of $E_{\perp}$ and $k_{//}$ and that $k_{//}$ filtering is a natural consequence of the situation, where an electron tunnels through a resonant state while its effective mass is changed. The filter characteristic of the GaAs-AlGaAs double barrier resonant tunneling structure is tremendously influenced by the thickness of the covering GaAs cap layer. The spectra shown in Fig. 5 are taken at the same sample at the positions A and B, as shown in Fig. 6.

By variation of the etch depth the transition between the steplike, $k_{//} = 0$, filter characteristic and the linear, $k_{//} >> 0$, filter characteristic can be investigated.

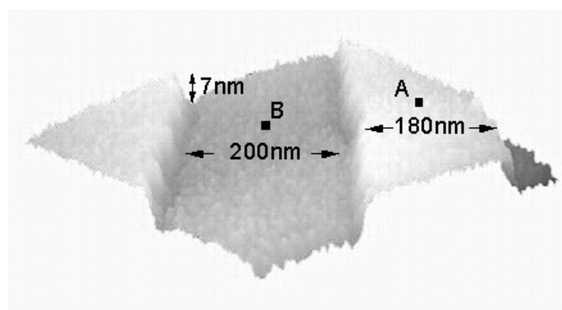

Fig. 6: STM based topographic image of the sample @ 4,2K. In the etched regions 3 nm GaAs, whereas in the unetched regions the initial 10 nm GaAs cap layer is remaining. The BEES data shown above are taken at point A on the wire and at point B in the valley.

3. A metal-insulator-metal injector for ballistic electron emission spectroscopy

(D. Rakoczy, R. Heer, G. Strasser, J. Smoliner)

As a supplement to STM (Scanning Tunneling Microscope) based BEES (Ballistic Electron Emission Spectroscopy) we have developed a solid-state version of BEES using a MIM (metal-insulator-metal) injector structure that replaces the tip of the STM. Our aim was to make an easy-to-fabricate, versatile and robust emitter for ballistic electrons.

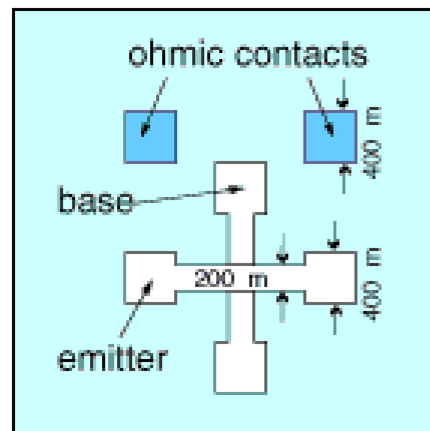

Fig. 7: Layout of the device.

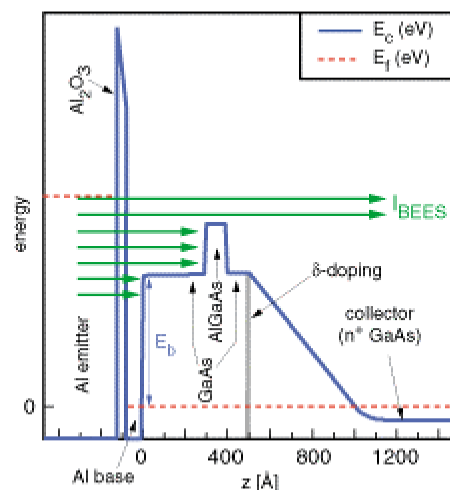

Fig. 8: MIM-Injector on a GaAs-AlGaAs-single barrier heterostructure: Schematic view of the conduction band profile and principle of ballistic electron injection.

The injector itself is realized by an Al-Al_2O_3-Al tunnel junction which is deposited on the structure under investigation. Up to now we concentrated our work on GaAs-AlGaAs heterostructures only, but of course the principle of a MIM injector for BEES can also be used for the investigation of other semiconductors. The size of a typical tunnel junction is 200 µm x 200 µm, but we did also some measurements using smaller

emitters. The design of our device allows an easy access to emitter, base, and collector and therefore is ideal for the simultaneous measurement of tunnel and BEES current with a quite simple setup. Moreover we can apply a bias voltage V_c (which is independent of the emitter voltage V_t used to provide the ballistic electrons) between base and collector and therefore "tilt" the band structure in the GaAs-AlGaAs.

To test our new emitter concept we investigated two different types of MBE grown GaAs-AlGaAs samples. The first (g218) consisted of GaAs only, while the other one (g232) had a single, 10 nm thick AlGaAs barrier 30 nm below the surface (the cap layer consisted of nominally undoped GaAs). Both samples were grown with a very thin region (just some atomic layers thick) of highly p-doped GaAs ("delta-doping") in the otherwise nominally undoped GaAs to provide a "flatband" condition at the surface.

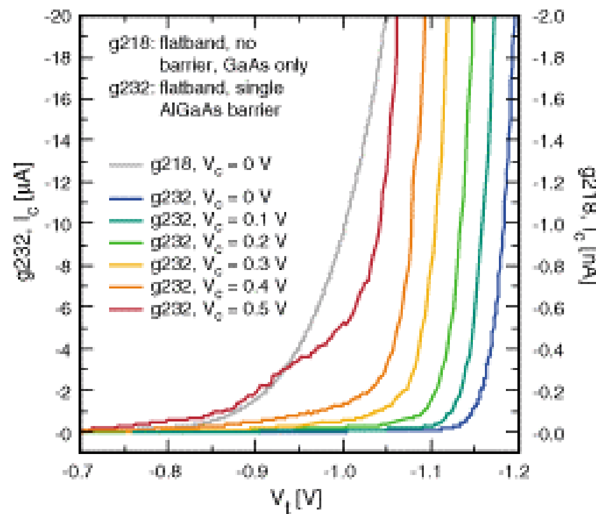

Fig. 9: Measured collector currents (Ic) on sample g232 for various collector voltages. The onset of the collector currents shifts in dependence of V_c. For higher collector voltages some leakage effects can be seen. For comparison also the (V_c = 0 V) collector current for sample g218 is shown.

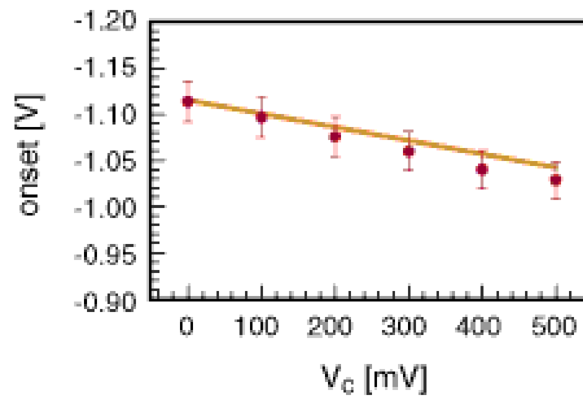

Fig. 10: Onset voltages of the collector current as a function of the applied collector voltage (V_c) for sample g232. The dots are experimental values extracted from the measured BEES spectra, the line shows the calculated behavior.

The measured onset voltages agree very well with the values expected from the band profile parameters. For V_c = 0 V we obtain a V_{onset} = –0.803 V for sample g218 and V_{onset} = –1.113 V for sample g232, respectively. The measured height of the AlGaAs barrier of g232 is thus 310 meV, in good agreement with the results obtained earlier on the same samples by STM-based BEES measurements. The shape of the BEES curves and the values of the onset voltages were reproduced on several samples and also agree excellently with the calculated results. On the other hand the total amount of the ballistic electron current shows large deviations when measured on different samples. This seems to originate in variations of the properties of the injector structures, i.e. especially the quality of the aluminum oxide barrier.

Applying a positive bias voltage to the collector electrode shifts the onset to smaller absolute values in V_t. This is exactly what is expected from the behavior of the band profile: $V_c > 0$ V means a lowering of the collector Fermi level which leads to a tilt of the band profile and therefore reduces the effective height of the AlGaAs barrier. The measured decrease in V_{onset} agrees quite well with results from self-consistent calculations. For higher collector bias values we observe some leakage effects.

4. Temperature dependent studies of InAs base layers for ballistic electron emission microscopy

(R. Heer, G. Strasser, J. Smoliner)

InAs is a promising new base material for ballistic electron emission microscopy (BEEM) since in this material, the attenuation length of ballistic electrons is more than one order of magnitude larger than for metal base layers and the corresponding transmission factor for ballistic electrons is strongly enhanced. Figure 11 shows a typical band diagram of a InAs-GaAs heterostructure with 240 nm thick InAs base layer.

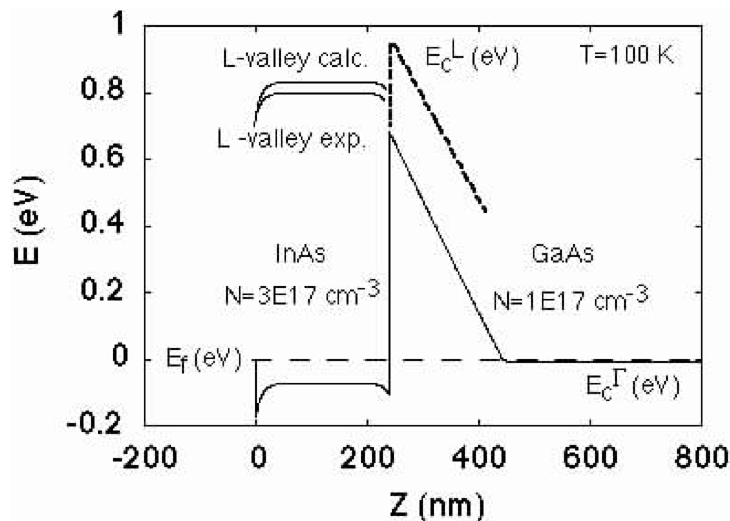

Fig. 11: Self consistently calculated band diagram of our InAs-GaAs heterostructure.

Unlike than other semiconductors, InAs has a surface accumulation layer of electrons and using the results of earlier magnetocapacitance and magnetotransport experiments, the Fermi level pinning at the surface is found to be 160 meV above the conduction

band. Figure 12 shows typical BEEM data of such a sample measured at temperatures of T = 100 K and T = 25 K, respectively. Obviously, the BEEM spectra are shifted to higher voltages with decreasing temperature.

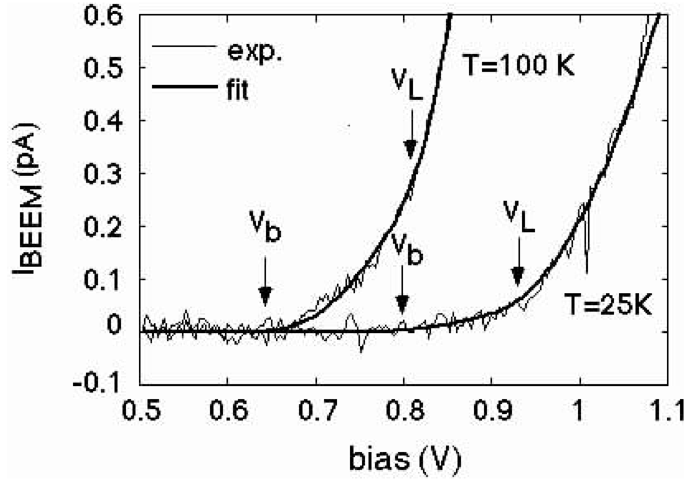

Fig. 12: Measured and calculated BEEM spectra at temperatures of T = 100 K and T = 25 K, respectively. The tunneling current was 1 nA, the InAs film thickness, 240 nm.

As shown previously, two different onset voltages can be identified in these BEEM spectra. The lower onset voltage, V_b, is the threshold voltage for ballistic electrons crossing the barrier at the InAs-GaAs interface in the Γ–valley. The second threshold at higher bias, V_L , corresponds to the onset of ballistic electron transport through the L-valley of the InAs film. The onset of ballistic electron transport through the X-valley of the InAs film would be expected 1 eV above the threshold for L-valley transport, which is outside the range of our measurement. To determine the onset voltages V_b and V_L and also the transmission factors for electrons traveling through the Γ and L valley, t_Γ and t_L, a modified Bell-Kaiser model was applied.

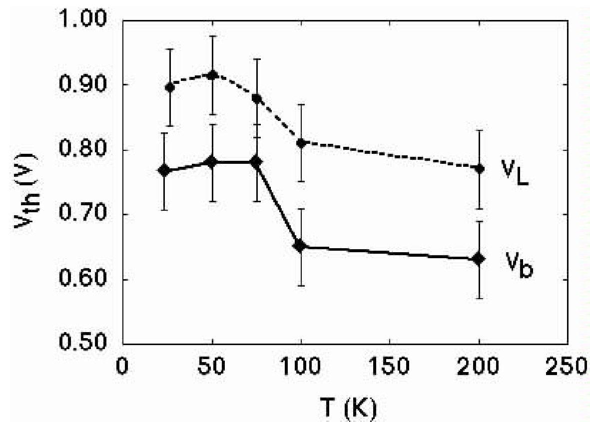

Fig. 13: Threshold voltages V_{th} as a function of temperature. V_b is the threshold voltage for the Γ valley, V_L the threshold for the L-valley. The variation of the threshold voltages determined on various sample positions was ± 0.06 V.

We now discuss the temperature behavior of the onset voltages V_b and V_L.

In Fig. 13, V_b and V_L are plotted as a function of temperature. Within the experimental errors, V_b and V_L increase equally with decreasing temperature. In addition, a steplike feature is revealed in the temperature curves around T = 100 K. Quantitatively, V_b and V_L increase by 160 meV in the temperature range between T = 200 K and T = 25 K. At T = 200 K and also when extrapolated to room temperature, the (Γ) barrier height at the InAs-GaAs interface on our samples agrees well with the data reported in the literature. A possible explanation for the large threshold shift around T = 100 K is a temperature dependent Fermi level pinning at the InAs-GaAs interface, however, we have no proof for this.

Our second major finding is somewhat surprising: With decreasing temperature, we find a decreasing base transmission for our InAs-GaAs heterostructures and InAs-GaAs heterostructures and we have verified this behavior on many different samples and also on different wafers. In Fig. 14 (a) we have plotted the temperature dependence of the transmission factors t_Γ and t_L for a 240 nm thick InAs film. Remarkably, the transmission decreases significantly with decreasing temperature. For the Γ valley, it decreases from 1.8% at T = 200 K to 0.35%, at T = 25 K. For the L valley, it decreases from 7% down to 1.5%. To get some information on the origin of this behavior, we have also made an Arrhenius plot of our data, which is shown in Fig. 14 (b). As one can see, the transmission shows a linear behavior when plotted on logarithmic scale as a function of (1/T). This behavior suggests a temperature activated transmission process, with an activation energy E_A^{Γ}= 4.9 ± 1 meV for the Γ and E_A^{L}= 5.3 ± 1 meV for the L-valley, respectively. The origin of this behavior is not understood at the moment, but we think that either temperature dependent scattering processes in the InAs and at the InAs-GaAs interface or traps can be made responsible for the observed effects.

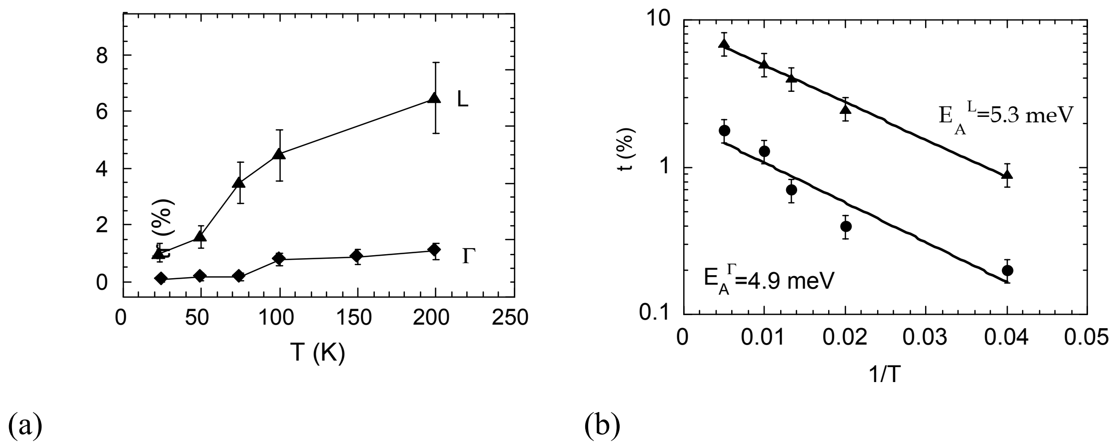

(a) (b)

Fig. 14: (a): Experimentally measured transmission factors for the Γ- and L-valley (t_Γ, t_L) as a function of temperature. Typically, the transmission factors varied by ≈18% across a sample. (b): Same data as a function of (1/T) plotted on a log-scale (Arrhenius plot).